OPTIMIZING THE NATURAL FREQUENCIES OF FUNCTIONALLY GRADED BEAMS AND ARCHES

George C. Tsiatas[1] and Aristotelis E. Charalampakis[2]

[1]School of Civil Engineering
National Technical University of Athens
Athens, GR-15773, Greece
e-mail: gtsiatas@gmail.com, web page: http://users.ntua.gr/gtsiatas

[2]Department of Civil Engineering
Gediz University
Izmir, 35665, Turkey
e-mail: aristotelis.charalampakis@gediz.edu.tr, web page: http://www.charalampakis.com/

Keywords: FGM, Heterogeneous material, Beams, Arches, Differential Evolution optimization.

Abstract. *In this paper a new design methodology is presented to optimize the natural frequencies of functionally graded beams and arches by tailoring appropriately their material distribution. The Functionally Graded Materials (FGMs) are deemed to have an advantageous behavior over laminated composites due to the continuous variation of their material properties yet in all three dimensions which eliminate delamination and crack initiation issues. The design of FGM structures is ideally fitted to optimization techniques, as the optimum material composition is derived by varying the relative volume fraction of the constituent materials. In this study the Differential Evolution (DE) is employed for optimizing the natural frequencies of FG beams and arches. The evaluation of the objective function requires the solution of the free vibration problem of an arch with variable mass and stiffness properties. The arches are modeled using a generic curved beam model that includes both axial (tangential) and transverse (normal) deformation and the problem is solved using the analog equation method (AEM) for hyperbolic differential equations with variable coefficients. The Mori and Tanaka homogenization scheme is adopted in this investigation for the estimation of the effective material properties. Several beams and arches are analyzed, which illustrate the design method and demonstrate its efficiency. In all cases three model problems are examined. We seek the material distribution that the FGM structure vibrates with (i) the maximum fundamental frequency, (ii) the minimum mass and the fundamental frequency greater than a prescribed value and (iii) the minimum mass and frequencies which lie outside certain frequency bands.*

1 INTRODUCTION

In this work a new design methodology is presented to optimize the natural frequencies of functionally graded beams and arches by tailoring appropriately their material distribution. The philosophy behind the concept of Functionally Graded Material (FGM) is to construct a heterogeneous composite which performs as a single-phase material, by unifying the best properties of its constituent phase materials. The FGMs are deemed to have an advantageous behavior over laminated composites due to the continuous variation of their material properties yet in all three dimensions which eliminate delamination and crack initiation issues. The design of FGM structures is ideally fitted to optimization techniques, as the optimum material composition is derived by varying the relative volume fraction of the constituent materials.

The endeavor to control the natural frequencies of a structure or structural element is a challenging and demanding task. By varying the mass and stiffness properties the design engineer seeks the structure to vibrate in accord to certain predefined criteria. This can be achieved via different types of structural optimization such as topology, shape or size [1], the detailed presentation of which is not the scope of this research. Besides the previous optimization techniques, the newly emerged FG materials have driven several researchers to address the so-called material volume fraction optimization. Qian and Batra [2] used a genetic algorithm together with a meshless local Petrov–Galerkin method and a higher-order deformable plate theory to find the compositional profile of a two-constituent cantilever plate so that either the first or the second natural frequency is maximum. In their work the volume fraction assumed to vary according a simple power law along the thickness and longitudinal direction. Goupee and Vel [3] also used a genetic algorithm to optimize the natural frequencies of functionally graded beams employing the element free Galerkin Method to analyze the free vibration problem. They treated the beam as a plane stress problem using a piecewise bicubic interpolation of volume fraction

specified at a finite number of grid points. In 2014, Alshabatat and Naghshineh [4] using an optimizer based on a genetic algorithm, determined the optimal profiles of volume fraction of beam constituent materials with the goal of maximizing the fundamental frequency which was computed via the Finite Element Method (FEM). In this paper they also presented two novel laws for describing the volume fractions through an FGM beam. The first one was a complex power law and the second one a trigonometric law.

A more complex optimization procedure for controlling the natural frequencies of FG materials has been proposed by some scholars. In this case, the simultaneous structural topology and material optimization has been addressed as a better alternative to the simple shape or material composition design. Rubio et al. [5], in 2011, presented a technique in order to achieve maximum and/or minimum vibration amplitudes at certain points of a structure, finding simultaneously the topology and material gradation function, whilst in 2014, Taheri and Hassani [6] developed a fully isogeometrical approach for the simultaneous shape and material composition design of FG structures to optimize their eigenfrequencies.

Although there have been a significant number of research papers on the analysis of the free vibration of FG arches [6]-[14], to the authors' knowledge, no work has been done on the design of FG arches for optimal natural frequencies. In our work the Differential Evolution (DE), a powerful metaheuristic algorithm, is employed for optimizing the natural frequencies of FG beams and arches. Nowadays, metaheuristic algorithms have emerged as the best way for solving complex optimization problems. These algorithms are usually inspired by evolution, swarm intelligence or physical phenomena principles and their widespread use is justified by a number of important advantages such as easy implementation, lack of dependency on gradient or other problem-specific information and good performance with global search characteristics [15].

The evaluation of the objective function requires the solution of the free vibration problem of an arch with variable mass and stiffness properties. The arch is modeled using a generic curved beam model that includes both axial (tangential) and transverse (normal) deformation, and is also able to account for variable mass and stiffness properties, as well as elastic support or restraint. The resulting dynamic governing equations of the circular arch are formulated in terms of the displacements and solved using an efficient integral equation method [18]-[20]. Moreover, for the estimation of the effective material properties of two-phase FG materials several homogenization methods have been proposed. The two foremost are the self-consistent [21] scheme and the Mori-Tanaka [22] scheme. The former has been originally introduced to compute the mechanical response of polycrystals and takes into account the interaction of the matrix and the grains using Eshelby's solution, while the latter has been proposed by Tanaka and Mori for composite materials involving only two phases and, it is assumed that the inclusions in the RVE, experience the matrix strain as the far-field strain in the Eshelby theory [23]. In this investigation the Mori and Tanaka [22] homogenization scheme is adopted for the estimation of the effective material properties. The method works well in instances where the microstructure consists of clearly defined matrix and particulate phases [3].

Several beams and arches are analyzed, which illustrate the design method and demonstrate its efficiency. In all cases three model problems are examined. We seek the material distribution that the FGM structure vibrates with (i) the maximum fundamental frequency, (ii) the minimum mass and the fundamental frequency greater than a prescribed value and (iii) the minimum mass and frequencies which lie outside certain frequency bands.

2 MODELLING AND NUMERICAL FORMULATION

2.1 Governing equations

Consider a plane curved beam the cross-sections of which are orthogonal to a plane curve (centroid axis) that belongs to the xz plane. A curvilinear abscissa s spans the curved beam's centroid axis which is vibrated under the combined action of the distributed loads $p_t = p_t(s)$ and $p_n = p_n(s)$ acting in the tangential and normal direction, respectively (see Figure 1). The curved beam may have a cross-section with variable properties, that is, the axial $EA(s)$ and bending stiffness $EI(s)$ vary due to heterogeneous linearly elastic material $E = E(s)$.

The differential equations of equilibrium are derived by considering the equilibrium of an elementary section in projections onto the tangential t and the normal n directions and in moments with respect to one of the beam's ends [24]. Taking also into account the inertia and damping forces, we arrive at the following equations of motion [20]

$$-m\ddot{u} - c\dot{u} + \left[EA\left(u_{,s} + \frac{w}{R} \right) \right]_{,s} = -p_t \tag{1}$$

$$-m\ddot{w} - c\dot{w} - \left[EI\left(w_{,ss} + \frac{w}{R^2} \right) \right]_{,ss} - \frac{1}{R}\left[EA\left(u_{,s} + \frac{w}{R} \right) + \frac{EI}{R}\left(w_{,ss} + \frac{w}{R^2} \right) \right] = -p_n \tag{2}$$

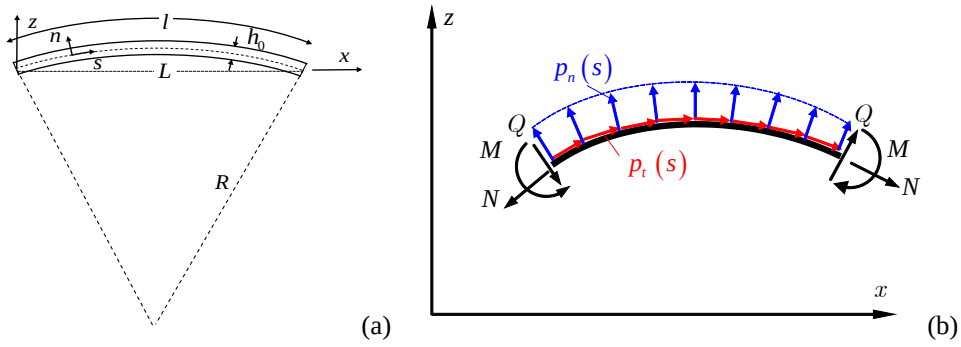

Figure 1. (a) Geometry of the arch and (b) positive forces and moments acting on a curved element.

where $m = m(s) = \rho A(s)$ is the mass density per unit length, c is the coefficient of viscous damping, R is the radius of the arch; $u(s)$ and $w = w(s)$ are the tangential and normal displacements, respectively.

The boundary conditions of the problem, that can include elastic support or restraint, are of the form

$$a_1 u(0,t) + a_2 N(0,t) = 0\,, \quad \bar{a}_1 u(l,t) + \bar{a}_2 N(l,t) = 0 \tag{3), (4}$$

$$\beta_1 w(0,t) + \beta_2 Q(0,t) = 0\,, \quad \bar{\beta}_1 w(l,t) + \bar{\beta}_2 Q(l,t) = 0 \tag{5), (6}$$

$$\gamma_1 \theta(0,t) + \gamma_2 M(0,t) = 0\,, \quad \bar{\gamma}_1 \theta(l,t) + \bar{\gamma}_2 M(l,t) = 0 \tag{7), (8}$$

where $a_k, \bar{a}_k, \beta_k, \bar{\beta}_k, \gamma_k, \bar{\gamma}_k$ $(k = 1,2)$ are given constants and $\theta = -w_{,s} + u/R$ is the slope of the cross-section. It is apparent that all types of the conventional boundary conditions (clamped, simply supported etc.) can be derived from Eqs. (3) - (8) by specifying appropriately these constants.

The stress resultants appear in the aforementioned equations are specified as [20]

$$N = EA\left(u_{,s} + \frac{w}{R}\right) + \frac{EI}{R}\left(w_{,ss} + \frac{w}{R^2}\right) \tag{9}$$

$$M = -EI\left(w_{,ss} + \frac{w}{R^2}\right) \tag{10}$$

$$Q = -EI\left(w_{,sss} + \frac{w_{,s}}{R^2}\right) - (EI)_{,s}\left(w_{,ss} + \frac{w}{R^2}\right) \tag{11}$$

Finally, the pertinent initial conditions of the problem are

$$u(s,0) = \tilde{u}(s)\,, \quad \dot{u}(s,0) = \dot{\tilde{u}}(s) \tag{12), (13}$$

$$w(s,0) = \tilde{w}(s)\,, \quad \dot{w}(s,0) = \dot{\tilde{w}}(s) \tag{14), (15}$$

where $\tilde{u}(s)$, $\dot{\tilde{u}}(s)$, $\tilde{w}(s)$ and $\dot{\tilde{w}}(s)$ are prescribed functions.

2.2 Free undamped vibrations

The equations of motion for the free undamped vibration model are derived from Eqs. (1) and (2) in the absence of external loading. That is,

$$-m\ddot{u} + \left[EA\left(u_{,s} + \frac{w}{R}\right)\right]_{,s} = 0 \tag{16}$$

$$-m\ddot{w} - \left[EI\left(w_{,ss} + \frac{w}{R^2}\right)\right]_{,ss} - \frac{1}{R}\left[EA\left(u_{,s} + \frac{w}{R}\right) + \frac{EI}{R}\left(w_{,ss} + \frac{w}{R^2}\right)\right] = 0 \tag{17}$$

2.3 Estimation of mechanical properties

In this investigation the Mori-Tanaka [22] homogenization scheme is adopted for the estimation of the effective material properties, for which there is overwhelming concurrence to yield realistic estimations of the material properties [1]. For this case, the effective bulk modulus $K(s)$ and shear modulus $G(s)$ are functions of the curvilinear abscissa s and expressed as [4]

$$\frac{K(s)-K_1}{K_2-K_1}=\frac{V_2}{1+3(1-V_2)(K_2-K_1)/(3K_1+4G_1)} \tag{18}$$

$$\frac{G(s)-G_1}{G_2-G_1}=\frac{V_2}{1+(1-V_2)(G_2-G_1)/(G_1+f_1)} \tag{19}$$

where

$$f_1=\frac{G_1(9K_1+8G_1)}{6(K_1+2G_1)} \tag{20}$$

and K_i, G_i and V_i ($i=1,2$) are the bulk modulus, shear modulus, and volume fraction of the constituent phase materials, respectively. It should be noted that for the volume fraction the relation $V_1+V_2=1$ always holds. Subsequently, the effective modulus of elasticity is determined as

$$E(s)=\frac{9K(s)G(s)}{3K(s)+G(s)} \tag{21}$$

while the effective mass density is given by the following rule of mixture

$$\rho(s)=\rho_1V_1+\rho_2V_2 \tag{22}$$

where ρ_i ($i=1,2$) are the mass densities of the constituent phase materials. In our analysis, and without restricting the generality, the FGM material is comprised of a steel phase (constituent $i=1$) and an aluminum phase (constituent $i=2$).

2.4 The AEM formulation

The evaluation of the objective function requires the solution of the free vibration problem of an arch with variable mass and stiffness properties. The initial boundary value problem described by Eqs. (16) and (17) together with the boundary conditions Eqs. (3) - (8) and the respective initial conditions Eqs. (12) - (15), is solved using the AEM [18]-[20], a robust numerical method based on an integral equation technique. Following Tsiatas and Fragiadakis [20] the analog equations for the problem at hand are

$$u_{,ss}=b_1(s,t) \tag{23}$$

$$w_{,ssss}=b_2(s,t) \tag{24}$$

The above equations describe the axial and bending linear response of an arch with constant unit axial and flexural stiffness subjected to the unknown fictitious axial b_1 and transverse b_2 loads, respectively, depending also in time. According to the AEM, the arch length l is divided into N equal elements (see Figure 2) on which the fictitious loads b_1 and b_2 are assumed constant.

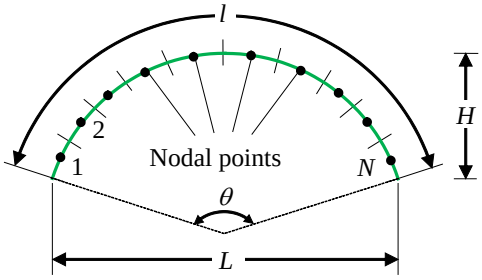

Figure 2. Arch geometry, discretization of the interval and distribution of the nodal points.

The discretized solution to Eqs. (23) - (24) including the respective derivatives are written as [20]

$$\{u\}=[T_1]\{b_1\},\quad \{u_{,s}\}=[T_{1s}]\{b_1\},\quad \{u_{,ss}\}=\{b_1\}, \tag{25), (26), (27}$$

$$\{w\}=[T_2]\{b_2\},\quad \{w_{,s}\}=[T_{2s}]\{b_2\}, \tag{28), (29}$$

$$\{w_{,ss}\}=[T_{2ss}]\{b_2\},\quad \{w_{,sss}\}=[T_{2sss}]\{b_2\},\quad \{w_{,ssss}\}=\{b_2\} \tag{30), (31), (32}$$

where $[T_1]$, $[T_{1s}]$, $[T_2]$, $[T_{2s}]$, $[T_{2ss}]$, $[T_{2sss}]$ are known $N\times N$ matrices accruing from the AEM implementation and $\{b_1\}$, $\{b_2\}$ vectors containing the N unknown time dependent nodal values of the fictitious

loads.

Furthermore, the first and second derivatives of the displacements with respect to time can be obtained by direct differentiation of Eqs. (25) and (28). That is,

$$\{\dot{u}\}=[T_1]\{\dot{b}_1\},\quad \{\ddot{u}\}=[T_1]\{\ddot{b}_1\}, \tag{33), (34}$$

$$\{\dot{w}\}=[T_2]\{\dot{b}_2\},\quad \{\ddot{w}\}=[T_2]\{\ddot{b}_2\} \tag{35), (36}$$

The final step of AEM is to apply Eqs. (16) and (17) to the N nodal points (see Figure 2) and substitute the displacements and their derivatives on the basis of Eqs. (25) - (32). Thus, we obtain the semi-discretized equation of motion

$$[M]\begin{Bmatrix}\{\ddot{b}_1\}\\ \{\ddot{b}_2\}\end{Bmatrix}+[K]\begin{Bmatrix}\{b_1\}\\ \{b_2\}\end{Bmatrix}=\begin{Bmatrix}\{0\}\\ \{0\}\end{Bmatrix} \tag{37}$$

with

$$[M]=\begin{bmatrix}[m_1] & [0]\\ [0] & [m_2]\end{bmatrix},\quad [K]=\begin{bmatrix}[k_{11}] & [k_{12}]\\ [k_{21}] & [k_{22}]\end{bmatrix} \tag{38), (39}$$

being the generalized mass, and stiffness matrix, respectively. The $N\times N$ known submatrices $[k_{11}]$, $[k_{12}]$, $[k_{21}]$, $[k_{22}]$ and $[m_1]$, $[m_2]$ are given by

$$[k_{11}]=-[EA]-[EA_s][T_{1s}] \tag{40}$$

$$[k_{12}]=-[EA]/R[T_{2s}]-[EA_s]/R[T_2] \tag{41}$$

$$[k_{21}]=[EA]/R[T_{1s}] \tag{42}$$

$$\begin{aligned}[k_{22}]=&\left([EA]/R^2+[EI]/R^4+[EI_{ss}]/R^2\right)[T_2]+\left([EI]/R^2+[EI_{ss}]\right)[T_{2ss}]\\ &+2[EI_s][T_{2sss}]+2[EI_s]/R^2[T_{2s}]+[EI]\end{aligned} \tag{43}$$

$$[m_1]=[\bar{\rho}][T_1] \tag{44}$$

$$[m_2]=[\bar{\rho}][T_2] \tag{45}$$

In Eqs. (40) - (45) $[EA]$, $[EA_s]$, $[EI]$, $[EI_s]$, $[EI_{ss}]$ being $N\times N$ diagonal matrices which contain the stiffness values and its derivatives at the N nodal values and $[\bar{\rho}]$ is a $N\times N$ diagonal matrix which contain the mass density per unit length at the N nodal values.

The associated initial conditions result from Eqs. (25) and (28) when combined with Eqs. (12) - (15). Thus, we have

$$\{b_1(s,0)\}=[T_1]^{-1}\{\tilde{u}(s)\},\quad \{\dot{b}_1(s,0)\}=[T_1]^{-1}\{\dot{\tilde{u}}(s)\} \tag{46), (47}$$

$$\{b_2(s,0)\}=[T_2]^{-1}\{\tilde{w}(s)\},\quad \{\dot{b}_2(s,0)\}=[T_2]^{-1}\{\dot{\tilde{w}}(s)\} \tag{48), (49}$$

For the free vibration case, we set

$$\{b_1(t)\}=\{B_1\}e^{-i\omega t} \tag{50}$$

$$\{b_2(t)\}=\{B_2\}e^{-i\omega t} \tag{51}$$

and Eq. (37) becomes

$$\left([K]-\omega^2[M]\right)\begin{Bmatrix}\{B_1\}\\ \{B_2\}\end{Bmatrix}=\begin{Bmatrix}\{0\}\\ \{0\}\end{Bmatrix} \tag{52}$$

giving a generalized eigenvalue problem of linear algebra, from which the eigenfrequencies ω and eigenvectors $\{B_1\}$, and $\{B_2\}$ are established. The eigenvectors may be used in Eqs. (25) and (28) to establish the mode shapes of the arch.

3 METAHEURISTIC OPTIMIZATION ALGORITHM

Differential Evolution (DE) is a stochastic optimization method that bears no natural paradigm. It was

introduced by Storn and Price [16] and an early version of the algorithm was initially conceived under the term "Genetic Annealing" [17]. In classic DE, usually denoted "rand/1/bin" [17], a population of P individuals is randomly dispersed within the design space, as

$$\begin{aligned} &\mathbf{x}_L \le \mathbf{x}_{i,0} \le \mathbf{x}_U \ \ \forall i \in \{1,2,...,P\} \\ &\mathbf{P}_{\mathbf{x},g} = \left(\mathbf{x}_{i,g}\right),\ i \in \{1,2,...,P\},\ g \in \{0,1,...,g_{\max}\} \\ &\mathbf{x}_{i,g} = \left(x_{j,i,g}\right),\ j \in \{1,2,...,D\} \end{aligned} \tag{53}$$

where $\mathbf{P}_{\mathbf{x},g}$ = array of P vectors (solutions); $\mathbf{x}_{i,g}$ = D-dimensional vector representing a candidate solution; $g_{\max}$ = maximum number of generations; i = index for vectors, g = index for generations, j = index for design variables; and the parentheses indicate an array. At each generation g, a mutated population $\mathbf{P}_{\mathbf{v},g} = \left(\mathbf{v}_{i,g}\right)$ is formed based on the current population $\mathbf{P}_{\mathbf{x},g}$, as

$$\mathbf{v}_{i,g} = \mathbf{x}_{r0,g} + F\left(\mathbf{x}_{r1,g} - \mathbf{x}_{r2,g}\right) \tag{54}$$

where, r_0, r_1 and r_2 are mutually exclusive random integers in $\{1,2,...,P\}$, which are also different from index i; $\mathbf{x}_{r0,g}$ = base vector; and F = a scalar parameter. After using Eq. (54), design variables are reset to their respective bounds in case a mutated solution moves out of the initial design space. Next, a trial population $\mathbf{P}_{\mathbf{u},g} = \left(\mathbf{u}_{i,g}\right)$ is formed, consisting of individuals created from the parent and mutated populations, as

$$\mathbf{u}_{i,g} = \left(u_{j,i,g}\right) = \begin{cases} v_{j,i,g}, \text{ if } \left(r \le C_r \text{ or } j = j_{rand}\right) \\ x_{j,i,g}, \text{ otherwise} \end{cases} \tag{55}$$

where, j_{rand} = a random index in $\{1,2,...,P\}$ that ensures that at least one design variable will originate from the mutant vector $\mathbf{v}_{i,g}$; and C_r = a scalar parameter in the range [0,1]. The final step of the algorithm is a greedy selection criterion, which for minimization problems is expressed as

$$\mathbf{x}_{i,g+1} = \begin{cases} \mathbf{u}_{i,g}, \text{ if } f\left(\mathbf{u}_{i,g}\right) \le f\left(\mathbf{x}_{i,g}\right) \\ \mathbf{x}_{i,g}, \text{ otherwise} \end{cases} \tag{56}$$

The above-described classic DE implementation usually demonstrates stronger exploration capability and thus is more suitable for solving multimodal problems [16]. Following recommendations in [17], $F = 0.5$ while a high value of $C_r = 0.9$ is expected to perform well with non-separable functions. The population size is set as $P = 50$ for all problems. In order to obtain reliable statistical data, 30 runs with different random seeds have been performed for each problem.

4 OPTIMIZATION EXAMPLES

On the basis of the numerical procedure presented in the previous section, a .NET code has been written and numerical results for FGM beams and arches have been obtained, which illustrate the applicability, effectiveness and accuracy of the proposed design methodology.

In this work, and without restricting the generality, we assume that the FGM constituents are steel and aluminum. Thus, we seek the material distribution for which a FGM structure vibrates with (i) the maximum fundamental frequency, (ii) the minimum mass and the fundamental frequency greater than a prescribed value and (iii) the minimum mass and frequencies which lie outside certain frequency bands. Following Alshabatat and Naghshineh [4], the volume fraction of material 1 (steel) is assumed to follow two alternative distributions, namely a four-parameter power law distribution (FGM-1)

$$V_1 = C\left[1 - \left(\frac{x}{L}\right) + a\left(\frac{x}{L}\right)^{\beta}\right]^{\gamma} \text{ for beams and } V_1 = C\left[1 - \left(\frac{s}{l}\right) + a\left(\frac{s}{l}\right)^{\beta}\right]^{\gamma} \text{ for arches,} \tag{57}$$

or a five-parameter trigonometric distribution (FGM-2)

$$V_1 = C\left[\frac{1}{2} - \frac{a}{2}\sin\left(\frac{\eta\pi x}{L} + \varphi\right)\right]^{\gamma} \text{ for beams and } V_1 = C\left[\frac{1}{2} - \frac{a}{2}\sin\left(\frac{\eta\pi s}{l} + \varphi\right)\right]^{\gamma} \text{ for arches.} \tag{58}$$

Note that the unknown parameters must be chosen so that $0 \le V_1 \le 1$ .The results are presented in terms of the non-dimensional frequency

$$\Omega_1 = \omega L^2 \sqrt{\frac{\rho_1 A}{E_1 I}} \text{ for beams and } \Omega_1 = \omega l^2 \sqrt{\frac{\rho_1 A}{E_1 I}} \text{ for arches,} \tag{59}$$

where A is the cross-sectional area, I is the second moment of area, L is the beam length, l is the developed arch length, ω is the natural frequency, and ρ_1 and E_1 are the density and modulus of elasticity of steel, respectively.

Both beams and arches under consideration have a length of $L = l = 1\text{m}$, width $b = 0.05\text{m}$, and thickness $h = 0.01\text{m}$, while $N = 51$ elements have been used for the discretization, unless stated otherwise. The properties of material 1 (steel) are E_1 = 210000 kN/m^2 and ρ_1 = 7.8 ton/m^3, whereas for material 2 (aluminum), E_2 = 70000 kN/m^2 and ρ_2 = 2.7 ton/m^3. The side constraints of the unknown parameters are set as $C_{\min}$ = 0, $C_{\max}$ = 1, $a_{\min}$ = 0, $a_{\max}$ = 1, $\gamma_{\min}$ = 0, $\gamma_{\max}$ = 15, $\beta_{\min}$ = 1, $\beta_{\max}$ = 15, $\eta_{\min} = -2$, $\eta_{\max}$ = 2, $\phi_{\min} = -\pi$, and $\phi_{\max} = \pi$. In order to produce valid statistical data, 30 runs with different random seeds have been executed for each problem.

4.1 Maximization of the fundamental frequency of a FGM beam

In this first example we investigate the problem of maximizing the fundamental frequency of FGM beams under various boundary conditions.

4.1.1 Fixed support – free end (cantilever)

The optimal design parameters which maximize the fundamental frequency are summarized in Table 1 and the distributions are shown in Figure 3. The non-dimensional frequencies reported in Ref. [4] were verified only when using an inaccurate central finite difference approach for the evaluation of the derivatives. A more robust evaluation of derivatives, based on the AEM, produces more accurate results, which is evident in Figure 3. Using the optimal material distribution based on the power law (FGM-1) shifts the frequency 18.44% and 20.70% higher than the frequency of a steel and an aluminum beam, respectively. The optimal material distribution based on the trigonometric law (FGM-2) shifts the frequency 29.29% and 31.76% higher than the frequency of a steel and an aluminum beam, respectively. Note that all runs converged to practically the same parameter values, i.e. the standard deviations are very small, which is an indication of a robust optimization process.

	Ω_1	C	α	Γ	β	η	φ
Pure steel	0.5596	-	-	-	-	-	-
Pure aluminum	0.5492	-	-	-	-	-	-
FGM-1 [4]	0.4926*	1.000	0.000	1.704	Any	-	-
FGM-1 (this study)	0.6628	1.000	1.000	2.042	15.000	-	-
FGM-2 [4]	0.6003*	1.000	1.000	1.601	-	1.304	-2.086
FGM-2 (this study)	0.7236	1.000	1.000	15.000	-	1.640	-0.524

(*) the results have been re-evaluated based on the given parameter values and discretization of 51 elements.

Table 1: Optimization results for the FGM cantilever.

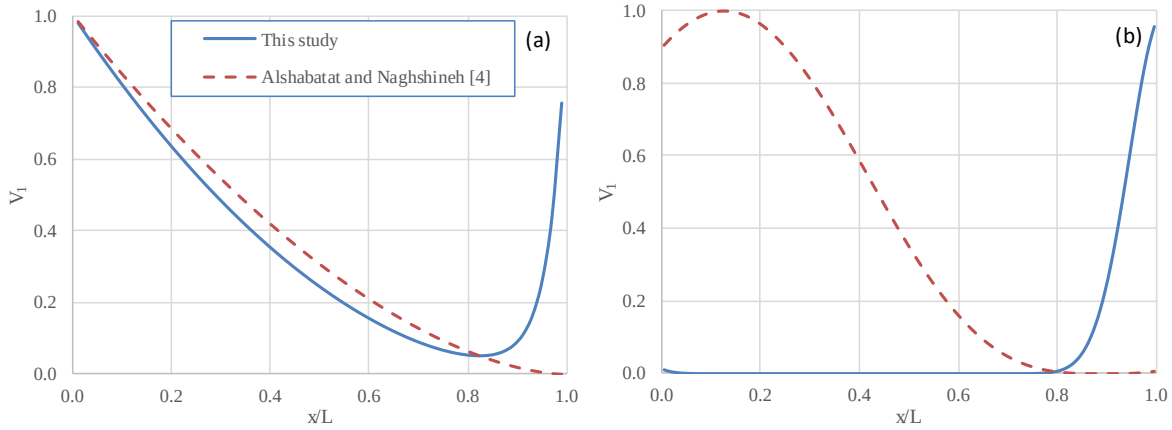

Figure 3. Optimum volume fraction of material 1 (steel) for a FGM cantilever (a) FGM-1 (b) FGM-2

4.1.2 Fixed – Fixed support (clamped beam)

The optimal design parameters which maximize the fundamental frequency are shown in Table 2, and the distributions are shown in Figure 4. Using the optimal material distribution based on the power law (FGM-1) shifts the frequency 15.52% and 17.72% higher than the frequency of a steel and an aluminum beam, respectively. The optimal material distribution based on the trigonometric law (FGM-2) shifts the frequency 28.28% and 30.73% higher than the frequency of a steel and an aluminum beam, respectively. Once again, all runs converged to practically the same parameter values. As an exception, the parameter η obtained a value of either +2 or -2. However, for mathematical reasons, this leads to the same distribution. For this symmetric problem, the difficulty of the power law (FGM-1) to provide symmetric distributions was profound. On the other hand, the trigonometric law (FGM-2) can naturally provide multiple symmetric alternatives due to the sine function, and thus was more suitable. Using the trigonometric law, the optimum distribution in Ref. [4] and the one found in this study are practically the same.

	Ω_1	C	α	γ	β	η	ϕ
Pure steel	3.5612	-	-	-	-	-	-
Pure aluminum	3.4946	-	-	-	-	-	-
FGM-1 [4]	4.0928*	1.000	1.000	11.010	2.066	-	-
FGM-1 (this study)	4.1137	1.000	1.000	7.358	2.944	-	-
FGM-2 [4]	4.5670*	1.000	1.000	2.833	-	1.998	-1.567
FGM-2 (this study)	4.5684	1.000	1.000	2.912	-	2.000	-1.571

(*) the results have been re-evaluated based on the given parameter values and discretization of 51 elements.

Table 2: Optimization results for the clamped FGM beam.

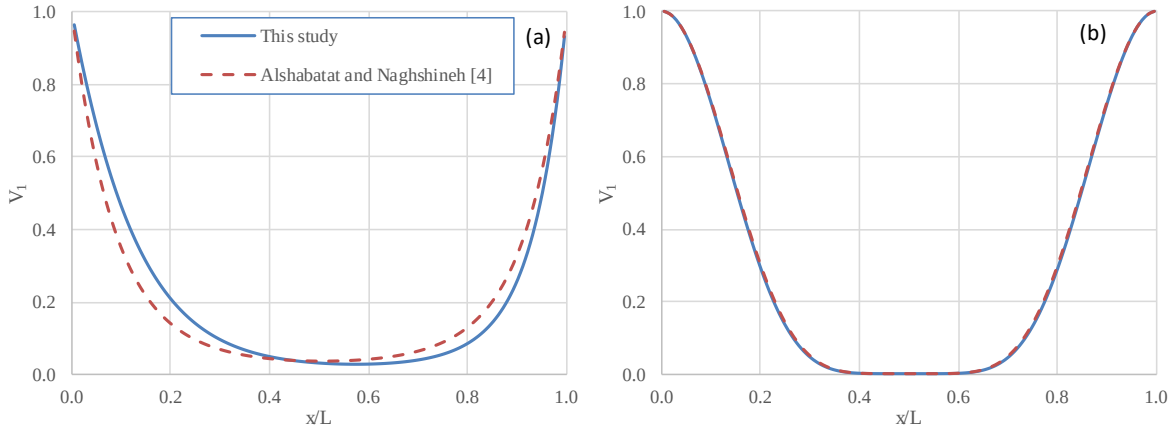

Figure 4. Optimum volume fraction of material 1 (steel) for a clamped FGM beam (a) FGM-1 (b) FGM-2

4.1.3 Fixed– Hinged support

Using the optimal material distribution based on the power law (FGM-1) shifts the fundamental frequency 11.61% and 13.74% higher than the fundamental frequency of a steel and an aluminum beam, respectively. The optimal material distribution based on the trigonometric law (FGM-2) shifts the fundamental frequency 17.94% and 20.19% higher than the fundamental frequency of a steel and an aluminum beam, respectively. The optimal design parameters are tabulated in Table 3, while in Figure 5 the optimum volume fraction distributions using both the power law (FGM-1) and the trigonometric law (FGM-2) are presented.

	Ω_1	C	α	γ	β	η	ϕ
Pure steel	2.4541	-	-	-	-	-	-
Pure aluminum	2.4082	-	-	-	-	-	-
FGM-1 (this study)	2.7391	1.000	1.000	5.476	15.000	-	-
FGM-2 (this study)	2.8943	1.000	1.000	15	-	-1.630	-2.712

Table 3: Optimization results for the FGM beam with fixed support – hinged support.

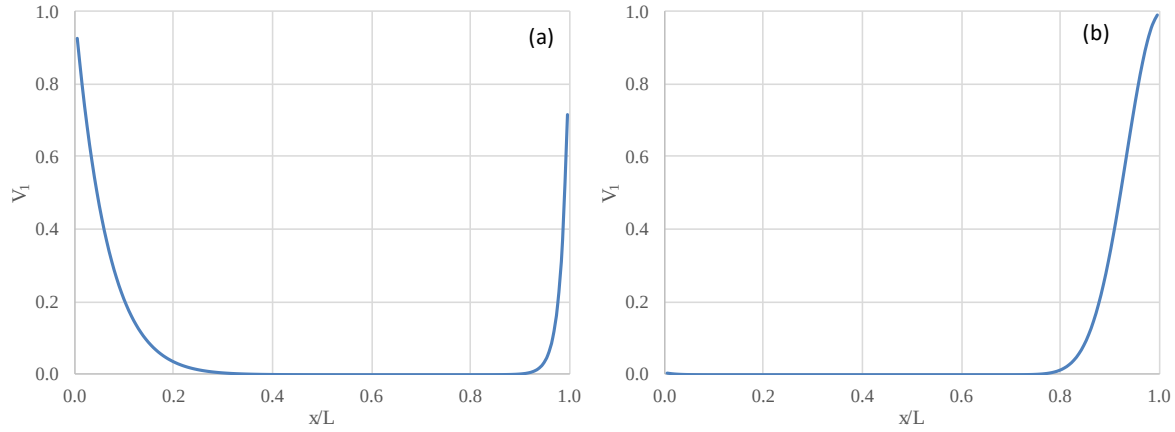

Figure 5. Optimum volume fraction of material 1 (steel) for a FGM beam with fixed support – hinged support (a) FGM-1 (b) FGM-2

4.1.4 Hinged– Hinged support

Using the optimal material distribution based on the power law (FGM-1) shifts the fundamental frequency 11.08% and 13.20% higher than the fundamental frequency of a steel and an aluminum beam, respectively. The optimal material distribution based on the trigonometric law (FGM-2) shifts the fundamental frequency 10.52% and 12.63% higher than the fundamental frequency of a steel and an aluminum beam, respectively. The optimal design parameters are tabulated in Table 4, while in Figure 6 the optimum volume fraction distributions using both the power law (FGM-1) and the trigonometric law (FGM-2) are presented.

	Ω_1	C	α	γ	β	η	ϕ
Pure steel	1.5709	-	-	-	-	-	-
Pure aluminum	1.5416	-	-	-	-	-	-
FGM-1 (this study)	1.7450	1.000	0.000	15	Any	-	-
FGM-2 (this study)	1.7362	1.000	1.000	15	-	-1.630	-2.712

Table 4: Optimization results for the FGM beam with hinged support – hinged support.

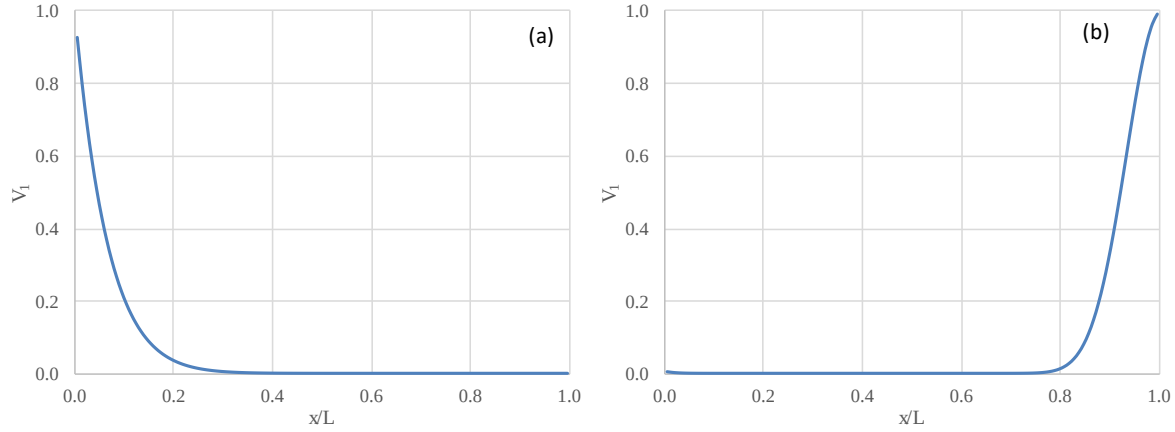

Figure 6. Optimum volume fraction of material 1 (steel) for a FGM beam with hinged support – hinged support (a) FGM-1 (b) FGM-2

4.2 Maximization of the fundamental frequency of a FGM clamped arch

In this second example the maximization of the fundamental frequency of a FGM clamped arch is investigated. Using the optimal material distribution based on the power law (FGM-1) shifts the fundamental frequency 8.94% and 11.01% higher than the fundamental frequency of a steel and an aluminum beam, respectively. The optimal material distribution based on the trigonometric law (FGM-2) shifts fundamental the frequency 15.38% and 17.58% higher than the fundamental frequency of a steel and an aluminum beam, respectively. The optimal design parameters are presented in Table 5, while in Figure 7 the optimum volume

fraction distributions using both the power law (FGM-1) and the trigonometric law (FGM-2) are shown. Particularly for Figure 7b, the optimum distribution is shown for $R = 2\,\mathrm{m}$ as well as the corresponding best results for the beam and the arch with $R = 100\,\mathrm{m}$. It is observed that the latter two almost coincide, as expected. Moreover, in Figure 8 the convergence curves of 30 independent runs of the FGM-2 distribution are depicted for the objective value ω, as well as parameter γ.

	Ω_1	C	α	γ	β	η	ϕ
Pure steel	9.7874	-	-	-	-	-	-
Pure aluminum	9.6044	-	-	-	-	-	-
FGM-1 (this study)	10.6621	1.000	1.000	12.281	2.540	-	-
FGM-2 (this study)	11.2927	1.000	1.000	8.213	-	2.000	-1.571

Table 5: Optimization results for the clamped FGM arch with $R = 2\,\mathrm{m}$

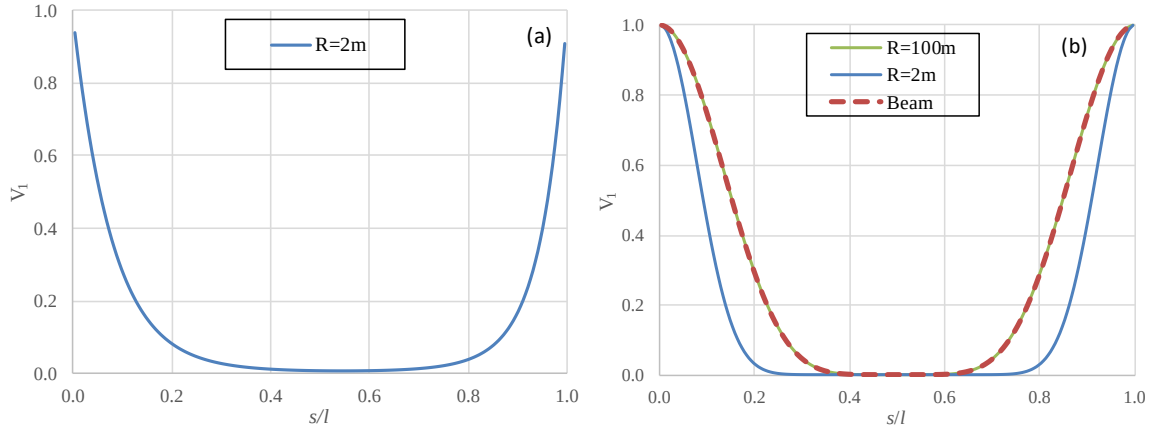

Figure 7: Optimum volume fraction of material 1 (steel) for a clamped FGM arch (a) FGM-1, (b) FGM-2

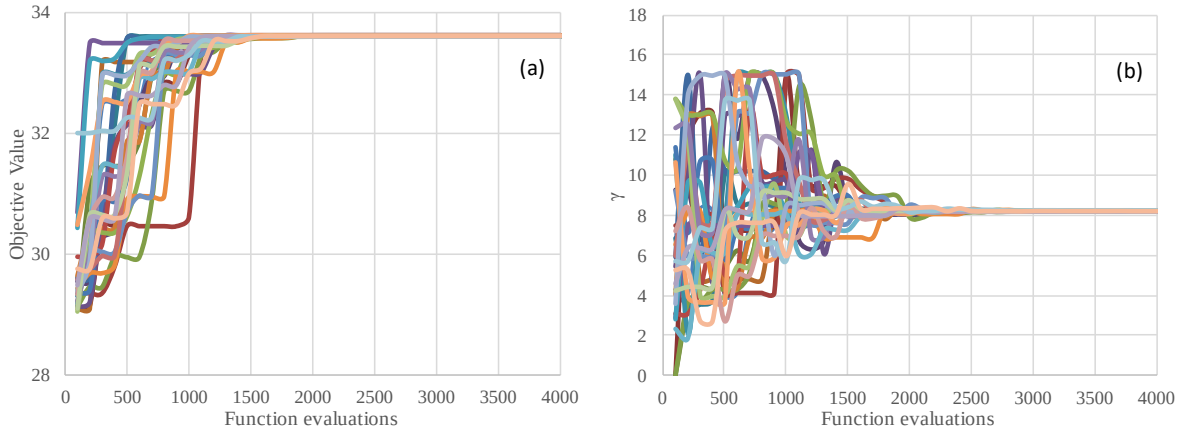

Figure 8: Convergence curves of 30 independent runs of the FGM-2 distribution for a clamped FGM arch with $R = 2\,\mathrm{m}$ (a) objective value ω, (b) parameter γ

4.3 Minimization of the mass while keeping the fundamental frequency equal or greater than a prescribed value for a FGM clamped arch

In this third example the minimization of the mass of a FGM clamped arch is investigated, while keeping its fundamental frequency greater than or equal to a prescribed value. This constraint is taken into account using the penalty method. Ideally, the penalty should be kept as low as possible, just above the limit below which infeasible solutions are optimal. This is called "the minimum penalty rule" and it is not particularly easy to implement. In this work, the penalty function takes the form

$$P(\mathbf{x}) = \sum_{j=1}^{N_c} \delta_j \left(A \times \left| g_j \right| + B \right) \tag{60}$$

where, $A = B = 10^{-3}$, N_c is the number of constraints, g_j is the j^{th} constraint and δ_j is an activation key defined as

$$\delta_j = \begin{cases} 0, & g_j \geq 0 \\ 1, & g_j < 0 \end{cases} \tag{61}$$

The constant term B is added when even the slightest violation occurs. This has proven to be very effective in keeping the best solutions free of penalties. In this example, $N_c = 1$ and the constraint takes the form

$$g_1(\mathbf{x}) = (\omega - 30) \geq 0 \tag{62}$$

Based on 30 independent runs, the optimal design parameters based on the trigonometric law (FGM-2) are $C = 1.000$, $a = 1.000$, $\eta = 1.701$, $\varphi = -1.096$ and $\gamma = 14.997$. The associated minimum total mass is ~ 0.00143 and the corresponding fundamental frequency is $\omega_1 = 30.000073$, which demonstrates that the constraint is active but no violation occurs. Figure 9a shows the convergence curves with respect to the objective value, i.e. the total mass. It is observed that all runs practically converge to the same optimum mass after less than 2000 function evaluations. Figure 9b shows the optimum distribution based on the trigonometric law (FGM-2) for $R = 2\,\text{m}$, as well as the corresponding best results for the beam and the arch with $R = 100\,\text{m}$. It is observed that the latter two almost coincide, as expected.

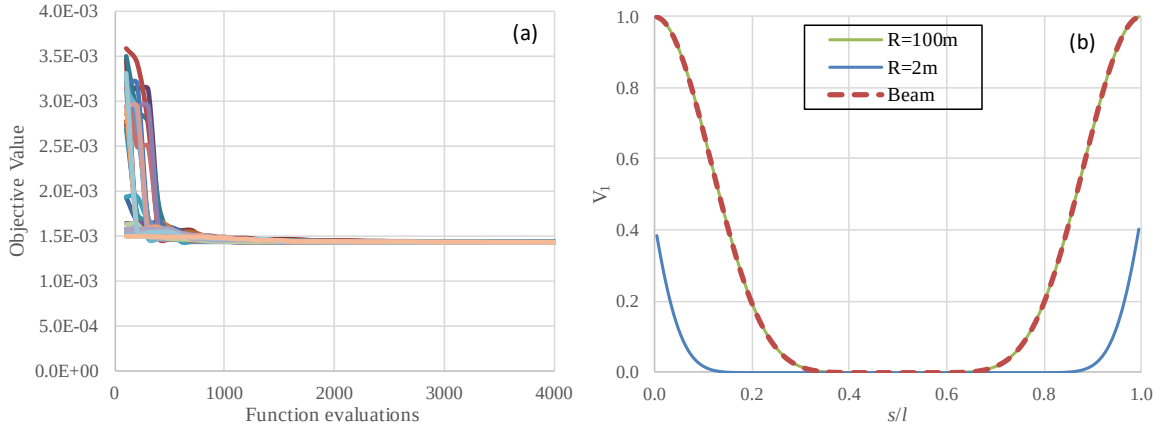

Figure 9: (a) Convergence curves of 30 independent runs of the FGM-2 distribution for a clamped FGM arch with respect to the objective value (total mass) (b) optimum FGM-2 distributions

4.4 Minimization of the mass while keeping all frequencies outside certain prescribed bands for a FGM clamped arch

In this last example the minimization of the mass of a FGM clamped arch is investigated, while keeping all its frequencies outside certain prescribed bands. Two frequency bands are used, namely from 28 to 35 and from 50 to 55, as

$$\begin{aligned} g_{2j-1}(\mathbf{x}) &= (\omega - 28)(\omega - 35) \geq 0 \\ g_{2j}(\mathbf{x}) &= (\omega - 50)(\omega - 55) \geq 0 \end{aligned} \tag{63}$$

The same penalty rule, given by Eq. (60), is used. Based on 30 independent runs, the optimal design parameters based on the trigonometric law (FGM-2) are $C = 0.883$, $a = 0.772$, $\eta = 1.942$, $\varphi = 2.906$ and $\gamma = 15$. The associated minimum total mass is ~ 0.001411 and the first three frequencies of the optimized FGM are $\omega_1 = 27.998086$, $\omega_2 = 49.996202$, and $\omega_3 = 92.248535$. Two of the first three frequencies, namely, ω_1 and ω_2, are right at the constraint boundaries, which again demonstrates that the constraints corresponding to the frequencies are active but no violation occurs. Figure 10a shows the convergence curves with respect to the objective value, i.e. the total mass. It is observed that all runs converge to practically the same optimum mass after 4000 function evaluations, with an average of 1.411E-03 and a standard deviation of 1.488E-06. The latter can be reduced further, if desired, by increasing the number of evaluations. On the other hand, a great variability in the parameter values was observed. For verification purposes, all 30 distributions are shown in Figure 10b. It is observed that, although the parameters of each design are significantly different, all distributions are

practically the same, featuring *one* hill which is placed symmetrically *either* at the left or at the right side of the arch.

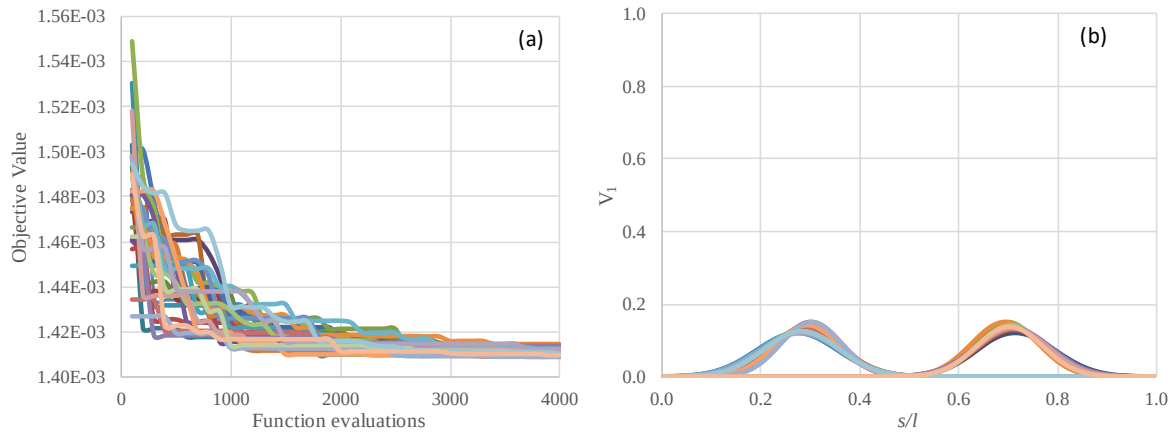

Figure 10: Results collected from 30 independent runs of the FGM-2 distribution for a clamped FGM arch with $R = 2\,\text{m}$ (a) Convergence curves with respect to the objective value (total mass) (b) Optimum distributions

5 CONCLUSIONS

In this paper a new design methodology was presented to optimize the natural frequencies of functionally graded beams and arches by tailoring appropriately their material distribution. Several beams and arches are analyzed, which illustrate the design method and demonstrate its efficiency. The main conclusions that can be drawn from this investigation are as follows:

- An integrated design methodology was presented for optimizing the natural frequencies of functionally graded beams and arches.
- The solution procedure of the free vibration problem of beams and arches with variable properties was achieved using the AEM. The method provides a direct solution of the differential equation of motion and overcomes the shortcoming of FEM solutions, which require resizing of the elements and recomputation of their stiffness and mass properties during the optimization process
- The Differential Evolution (DE), has been proven to be a powerful metaheuristic algorithm which is able to quickly discover the optimum distributions based on the selected objective function and the constraints. It has demonstrated a robust behavior and the selected computational budget, i.e. 4000 function evaluations, is sufficient for the complexity of the problem at hand.
- For symmetric problems, the four-parameter power law distribution (FGM-1) has been proven incapable to provide symmetric material distributions.
- In contrast, the five-parameter trigonometric distribution (FGM-2) generates symmetric material distributions for symmetric problems.
- Moreover, in all cases the FGM-2 distribution produces better results except for the hinged-hinged beam in Example 4.1.1.
- The design methodology yields the same material distribution in examples 4.1.3 and 4.1.4 using FGM-2 distribution.
- Overall, the FGM-2 distribution exhibits superior behavior over FGM-1 and is nominated, between the two examined, for the design of FGM beams and arches for optimum frequency response.

REFERENCES

[1] Taheri, A.H. and Hassani, B. (2014), “Simultaneous isogeometrical shape and material design of functionally graded structures for optimal eigenfrequencies,” Comput. Methods Appl. Mech. Engrg. 277, pp. 46–80.
[2] Qian, L.F. and Batra, R.C. (2005), “Design of bidirectional functionally graded plate for optimal natural frequencies,” J. Sound and Vib. 280, pp. 415–424.
[3] Goupee, A.J. and Vel, S.S. (2006), “Optimization of natural frequencies of bidirectional functionally graded beams,” Struct. Multidisc. Optim. 32, pp. 473–484.
[4] Alshabatat, N.T. and Naghshineh, K. (2014), “Optimization of natural frequencies and sound power of beams using functionally graded material,” Adv. Acoust. Vib., Article ID 752361.
[5] Rubio, W.M., Paulino, G.H. and Silva, E.C.N. (2011), “Tailoring vibration mode shapes using topology optimization and functionally graded material concepts,” Smart Mater. Struct. 20, 025009.

[6] Lim, C.W., Yang, Q., Lü, C.F. and Xu, R. (2009), "Two-dimensional elasticity solutions for temperature-dependent in-plane vibration of FGM circular arches," Compos. Struct. 90, pp. 323–329.
[7] Malekzadeh, P. (2009), "Two-dimensional in-plane free vibrations of functionally graded circular arches with temperature-dependent properties," Compos. Struct. 91, pp. 38–47.
[8] Malekzadeh P., Atashi, M.M. and Karami, G. (2009), "In-plane free vibration of functionally graded circular arches with temperature-dependent properties under thermal environment," J. Sound Vib. 326, pp. 837–851.
[9] Filipich, C.P. and Piovan, M.T. (2010), "The dynamics of thick curved beams constructed with functionally graded materials," Mech. Res. Commun. 37, pp. 565–570.
[10] Yousefi, A. and Rastgoo, A. (2011), "Free vibration of functionally graded spatial curved beams," Compos. Struct. 93, pp. 3048–3056.
[11] Piovan, M.T., Domini, S. and Ramirez, J.M. (2012), "In-plane and out-of-plane dynamics and buckling of functionally graded circular curved beams," Compos. Struct. 94, pp. 3194-3206.
[12] Wu, J.S., Lin, F.T. and Shaw, H.J. (2013), "Free in-plane vibration analysis of a curved beam (arch) with arbitrary various concentrated elements," Appl. Math. Model. 37, pp. 7588-7610.
[13] Rajasekaran, S. (2013), "Static, stability and free vibration analysis of arches using a new differential transformation-based arch element," Int. J. Mech. Sci. 77, pp. 82–97.
[14] Eroglu, U. (2015), "In-plane free vibrations of circular beams made of functionally graded material in thermal environment: Beam theory approach," Compos. Struct. 122, pp. 217–228.
[15] Eiben, A.E., Smith, J.E. (2003), *Introduction to evolutionary computing*, Springer-Verlag, New York.
[16] Storn, R. and Price, K. (1997), "Differential evolution – a simple and efficient heuristic for global optimization over continuous spaces," J. Global Optim. 11, pp. 341–359.
[17] Storn, R., Price, K., Lampinen, J.A. (2005), *Differential evolution – a practical approach to global optimization*, Springer-Verlag.
[18] Katsikadelis, J.T. and Tsiatas, G.C. (2004), "Non-linear dynamic analysis of beams with variable stiffness," J. Sound and Vib. 270, pp. 847–863.
[19] Katsikadelis, J.T. and Tsiatas, G.C. (2006), "Regulating the vibratory motion of beams by shape optimization", J. Sound Vib. 292, pp. 390-401.
[20] Tsiatas, G.C. and Fragiadakis, M. (2015), "Seismic response and design of arched structures," *Proceedings of the 9th GRACM International Congress on Computational Mechanics*, Volos, Greece, 12 – 15 July, Book of Abstracts pp. 113.
[21] Hill, R. (1965), "A self-consistent mechanics of composite materials," J. Mech. Phys. Solids 13, pp. 213–222.
[22] Mori, T. and Tanaka, K. (1973), "Average stress in matrix and average elastic energy of materials with misfitting inclusions," Acta Metall. 21, pp. 571–574.
[23] Perdahcıoğlu, E.S. and Geijselaers, H.J.M. (2011), "Constitutive modeling of two phase materials using the mean field method for homogenization," Int. J. Mater. Form. 4, pp. 93–102.
[24] Slivker, V. (2007), *Mechanics of Structural Elements, Theory and Applications*, Springer-Verlag Berlin Heidelberg.